y scaling in quasifree pion-single-charge exchange

R. J. Peterson,[1] C. E. Allgower,[2] V. Bekrenev,[3] W. J. Briscoe,[4] J. R. Comfort,[5] K. Craig,[5] D. Grosnick,[6] D. Isenhower,[7] N. Knecht,[8] D. Koetke,[6] A. A. Kulbardis,[3] G. Lolos,[8] V. Lopatin,[3] D. M. Manley,[9] R. Manweiler,[6] A. Marušić,[10] S. McDonald,[11] B. M. K. Nefkens,[12] J. Olmsted,[9,*] Z. Papandreou,[8] D. C. Peaslee,[13] N. Phaisangittisakul,[12] J. Price,[12] D. E. Prull,[1] A. F. Ramirez,[5] M. Sadler,[7] A. Shafi,[4] H. Spinka,[14] T. D. S. Stanislaus,[6] A. Starostin,[12] H. M. Staudenmaier,[15] I. Strakovsky,[4] and I. Supek[16]

(Crystal Ball Collaboration)

[1]*University of Colorado, Boulder, Colorado 80309-0390, USA*
[2]*Indiana University Cyclotron Facility, Bloomington, Indiana 47405, USA*
[3]*Petersburg Nuclear Physics Institute, Gatchina RU-188350, Russia*
[4]*The George Washington University, Washington, DC 20052-0001, USA*
[5]*Arizona State University, Tempe, Arizona 85287, USA*
[6]*Valparaiso University, Valparaiso, Indiana 46383-6493, USA*
[7]*Abilene Christian University, Abilene, Texas 79699-7963, USA*
[8]*University of Regina, Saskatchewan, Canada S4S OA2*
[9]*Kent State University, Kent, Ohio 44242-0001, USA*
[10]*Collider-Accelerator Department, Brookhaven National Laboratory, Upton, New York 11973, USA*
[11]*TRIUMF, 4004 Wesbrook Mall, Vancouver, Canada V6T 2A3*
[12]*University of California Los Angeles, Los Angeles, California 90095-1547, USA*
[13]*University of Maryland, College Park, Maryland 20742-4111, USA*
[14]*Argonne National Laboratory, Argonne, Ilinois 60439-4815, USA*
[15]*Universitat Karlsruhe, Karlsruhe 76128, Germany*
[16]*Rudjer Boskovic Institute, Zagreb 10002, Croatia*

(Received 25 April 2003; published 18 June 2004)

Data for pion-single-charge exchange reactions at 750 MeV/*c* on complex nuclei are analyzed for *y*-scaling, or single scattering quasifree, responses. The angular dependence of the data is used to separate the spin and nonspin isovector responses, with comparisons to electron scattering results.

DOI: 10.1103/PhysRevC.69.064612 PACS number(s): 25.80.Gn, 25.80.Ls

I. INTRODUCTION

Electron scattering experiments have shown that incoherent single-nucleon elastic scattering on bound nucleons within complex nuclei can be demonstrated by kinematic considerations, via the mechanism of *y* scaling [1]. This method has also been applied to quasifree (non-charge-exchange) pion scattering (NCX) data, where *y* scaling is also found, after taking into account distortion, shadowing, and second-scattering effects, at least for light nuclei [2]. The scaling responses found for the pion beam differed from those found with electrons. Here we apply a similar *y*-scaling analysis to quasifree pion-single-charge exchange (SCX) data at a beam momentum of 750 MeV/*c*. We expect strong interaction effects to cause our isovector scaling to differ from that seen with electrons. If the general characteristics of *y*-scaling are seen in SCX, we may use the single scattering to infer changes in the pion-nucleon SCX cross sections in the nuclear interior, relative to those in free space.

We use the portion of the continuous spectrum of the scattered neutral meson near the kinematics for the free SCX scattering. The beam momentum and momentum transfers suffice to meet the conditions of incoherent scattering at all except the smallest angles [3].

The kinematic *y*-scaling methods are described in Sec. II, including the changes from the standard usage because of the charge-changing nature of the reaction. As in the NCX analysis, the SCX data must be corrected for effects of the large meson-nucleon cross sections. This is carried out as described in Sec. II, with a test of the results in Sec. III. Measured cross sections shown in Sec. III are fit to obtain the in-medium meson-proton charge exchange differential cross sections, and the doubly differential cross sections are subjected to the *y*-scaling transformation. Scaling is found not to be valid under the simplest assumptions, and the response data are compared to a new spin separation analysis in Sec. IV. The special case of quasifree pion SCX on the deuteron is treated in Sec. V, and the results of our analysis for all nuclei are compared to the conclusions from electron scattering in Sec. VI.

II. METHODS

The *y*-scaling analysis assumes that there has been one and only one quasifree elastic collision (here, free charge exchange by a π^- beam on a target proton) of the projectile with a bound nucleon, which will have some distribution of its momentum. These assumptions allow the combination of

*Present address: Midwest Proton Radiotherapy Institute, Bloomington, IN 47405.

TABLE I. Several parameters used in the present analysis of pion SCX spectra are presented. Fermi momenta k_F were obtained from the widths of the quasifree peaks in the 45° and 55° SCX spectra, using a relativistic Fermi gas model.

Nucleus	SE (MeV)	k_F (MeV/c)	Z_{eff}
D	−2		1.0
C	11	235	1.722
Al	8	231	2.786
Cu	6	277	3.935

the two variables q (the laboratory frame three-momentum-transfer to the projectile) and ω (the laboratory frame energy loss of the projectile) to be combined into a single variable, y, which may be thought of as the component of the nucleon internal momentum along the direction of the momentum transfer, for large values of q [1]. If the assumptions and parameters are correct, all measured doubly differential cross sections will yield the same value for a certain transformed spectral observable.

We use the kinematic variable

$$y = y_\infty \left[1 - \frac{y_\infty \sqrt{M^2 + (q_{\text{eff}} + y_\infty)^2}}{2M(A-1)(y_\infty + q_{\text{eff}})} \right] \tag{1}$$

for a target of mass A, including recoil [4], with

$$y_\infty = \sqrt{(\omega - \text{SE})^2 + 2M(\omega - \text{SE})} - q_{\text{eff}}. \tag{2}$$

The separation energy parameters SE are taken to be those used by Ref. [4], with the inclusion of the Coulomb energy for the negative pion beam and of the free SCX Q value of 3.8 MeV. These are listed in Table I. The effective momentum transfer is used to include the Coulomb effect on the π^- beam, as in Ref. [2]. The nuclear potential sensed by the projectile will also change the effective momentum transfer. Real potential well depths obtained from fits to π-carbon elastic scattering near 750 MeV/c are small (about 8 MeV and attractive) [5], and so the effect of this interaction is not included here. Free nucleon masses M are used throughout in the present work.

The measured doubly differential cross sections are transformed into

$$F(y) = \frac{d^2\sigma/d\Omega\, d\omega}{d\ \sigma/d\Omega(\text{free})} \frac{1}{Z_{\text{eff}}} \frac{q_{\text{eff}}}{\sqrt{M^2 + (y + q_{\text{eff}})^2}} \tag{3}$$

using the free proton pion SCX cross sections measured during the same experiment, with the same angle bins and energy resolution. No effects of internal momentum distributions in the complex nuclei were included. Note that several systematic uncertainties cancel with this usage. The number of protons in the target nucleus eligible for strictly single scattering (Z_{eff}) is computed by an eikonal or Glauber method [6] based upon compiled pi-nucleon total cross sections [7] and using distributions of protons from Ref. [8]. Since the response $F(y)$ does scale for electron scattering on nuclei, it is our goal to use the SCX scaling functions to infer $d\sigma/d\Omega$, not free, but within nuclei.

Meson-nucleon total cross sections for π^- were used in this computation of Z_{eff}; note that charge symmetry implies that the average π^0 total cross sections are the same as those for π^- in a symmetric nucleus. These total cross sections, and hence Z_{eff}, change little with the energy of the outgoing particle until outgoing energies are near 180 MeV. This is reached for the quasifree peak at 750 MeV/c only at angles of 155° and beyond. Meson-carbon total cross sections computed with this model were shown to agree with measured values to within about 10% in Ref. [2].

The validity of this Z_{eff} computation was demonstrated by the test of superscaling in Ref. [2], where the scaling responses $F(y)$ were transformed by the nuclear Fermi motion into a response $f(Y)$ that should be the same for all nuclear targets, as examined for electron scattering [4]. This transformation is here applied to SCX data.

The superscaling comparisons are then for

$$Y = y/k_F \tag{4}$$

and

$$f(Y) = k_F F(y). \tag{5}$$

Strictly speaking, superscaling should require both y scaling for each target for a range of q or θ, and Y scaling for each target at each q. If medium effects alter the elementary SCX differential cross section from angle to angle, the mass dependent part of superscaling might still be expected to hold at a given angle. We shall use superscaling in the latter sense, as a test of the Z_{eff} method. The Fermi momenta k_F for this superscaling analysis are taken from the measured widths of the SCX spectra at 45° and 55°, averaged using the relativistic Fermi gas model as in Ref. [4]. Results are listed in Table I; uncertainties are about 10 MeV/c.

III. DATA AND RESULTS

The cross sections presented here for a π^- beam momentum of 750 MeV/c were obtained with a detector subtending nearly 4π of solid angle. The experiment used the Crystal Ball detector and π^- beam from the Brookhaven AGS; some results from this same experiment were presented in Ref. [9].

The large acceptance of 93% of 4π allows us to select π^0 events decaying to only two photons, and the spectra are thus exclusive, with one and only one (almost) π^0 ejectile. A charged particle veto counter was also used, further emphasizing the exclusive SCX reaction. Normalization of the cross sections, after efficiency corrections by a Monte Carlo system described in Ref. [9], was checked by comparison to our proton SCX yield, obtained by subtraction using CH_2 and C samples, to the phase-shift expectations for SCX [7].

Since the coverage of the Crystal Ball Detector was so broad, we show in Fig. 1 the relation between angles, energies, and three-momentum-transfers. The data were binned into 10° segments, nearly corresponding to a fixed momentum transfer for each bin.

Samples of the obtained doubly differential cross sections are shown in Figs. 2–4. Gaussian fits to the quasifree peaks

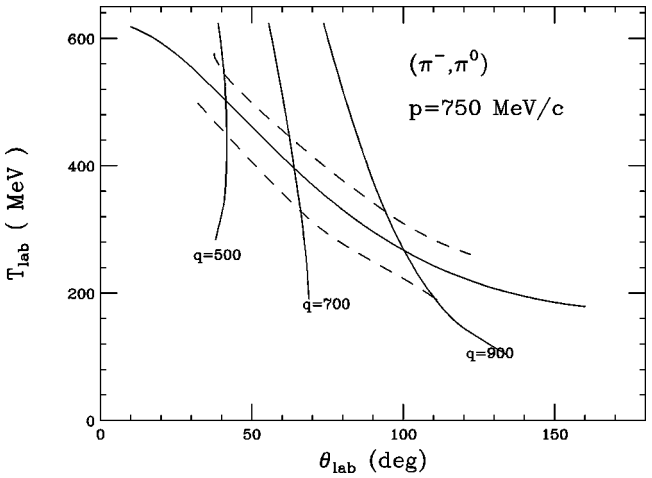

FIG. 1. The angular coverage of the Crystal Ball detector ranges from 25° to 155°. The locus of free pion SCX is shown by the solid curve; this will lie near the values of $y=0$ for the complex target spectra. Dashed lines show where y is to be found 100 MeV/c from this center. Labeled curves show loci of fixed free three-momentum-transfer, in MeV/c.

are formed by forcing agreement to the high laboratory energy side without a background, as shown in these figures. A linear background was estimated as indicated in these samples to yield singly differential cross sections and quasifree responses above that background. Uncertainties for these subtracted results were taken to be one-third of the background. These backgrounds could be due to a number of processes other than single scattering not removed by our nearly exclusive trigger. Angle bins are taken to be 10° wide, and are available from 25° to 155°, covering a laboratory momentum-transfer range from 431 to 1004 MeV/c for free scattering. The SCX inclusive spectra at 624 MeV/c show a

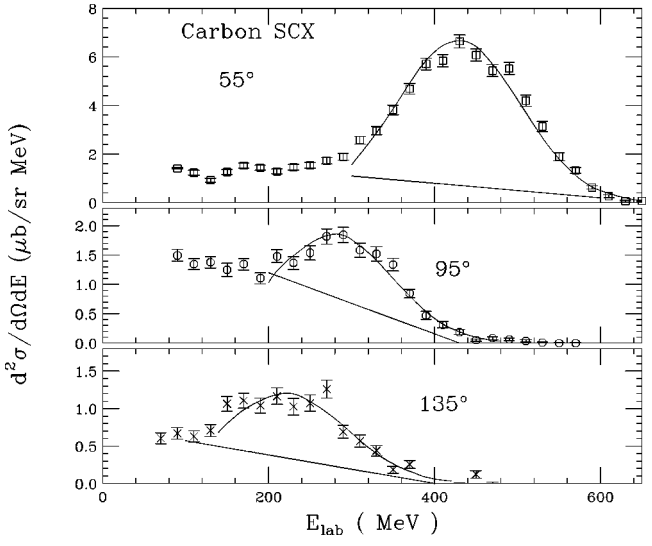

FIG. 2. Doubly differential (π^-,π^0) cross sections from the Crystal Ball at 750 MeV/c are shown for carbon. The curves show fits based upon the assumption of no background and using the high energy edge of the quasifree peak; a linear background as indicated was used for some results.

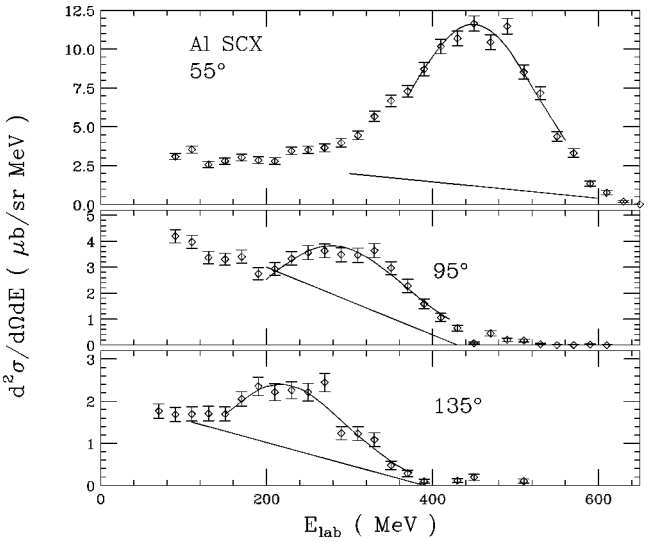

FIG. 3. As for Fig. 2, but for the aluminum target.

strong rise at moderate angles for large energy losses [10] unlike the present exclusive data.

Spectra from 45° for C, Al, and Cu are shown in Fig. 5 as transformed to the superscaling format, with Fermi momenta and $Z_{\rm eff}$ values as listed in Table I. These match well, confirming the validity of the $Z_{\rm eff}$ method for the magnitudes of our scaling responses at forward angles. This same conclusion was reached for pion NCX on complex light nuclei at 950 MeV/c [2]. The laboratory momentum transfer for free scattering at 750 MeV/c and 45° is 534 MeV/c.

The fits with backgrounds enable integrated singly differential cross sections to be formed, after division by $Z_{\rm eff}$. These areas used the fitted high energy edge of the peak to define a Gaussian, with the linear background estimated across the entire peak, as indicated in Figs. 2–4. Peak areas without backgrounds gave differential cross sections in agreement with those shown in Ref. [9], lying between the open and closed points in their Fig. 10, where different fitting

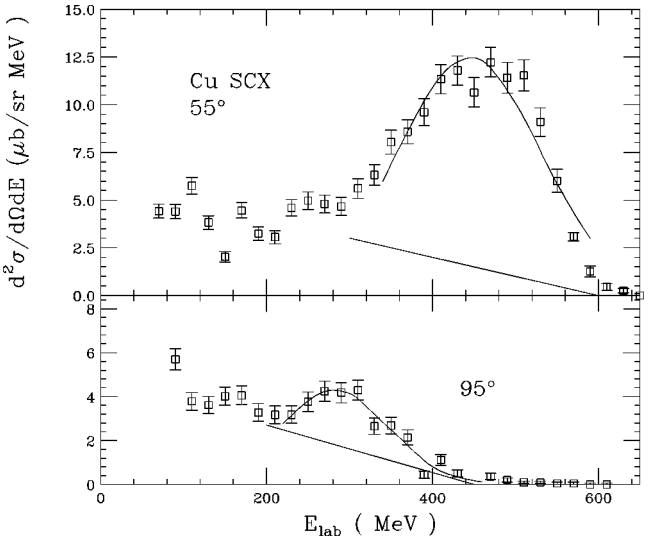

FIG. 4. As for Fig. 2, but for the copper target. The spectrum at 135° had too few counts to be useful.

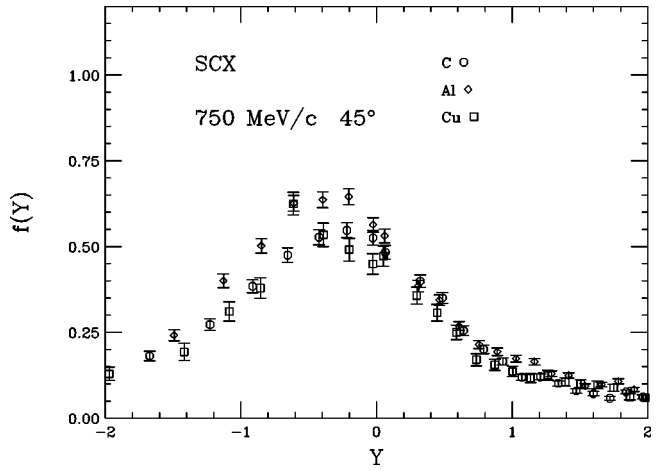

FIG. 5. Cross sections as in Figs. 2–4 without background subtraction are shown at 45° for the three complex targets, after transformation to the superscaling format. The parameters of the transformation are listed in Table I. This agreement for three target nuclei is taken to indicate the validity of our method to determine Z_{eff}, which changes from 1.7 to 3.9 for this range of nuclei. The momentum transfer q of 530 MeV/c for these data is near the values emphasized in the π^- NCX cases in Ref. [2].

systems were used to measure the areas of the quasifree peaks. The arbitrary units used in Ref. [9] were converted to mb/sr by means of the comparison of the relative free-space cross sections ($d\sigma/d\Omega$) shown in Fig. 6 to actual free SCX cross sections [7]. These quasifree SCX cross sections for complex targets differ significantly from the expected free scattering.

The exclusive single π^0 trigger used for the Crystal Ball measurement provides a clear peak near $y=0$ out to large scattering angles. The example for the carbon target is shown

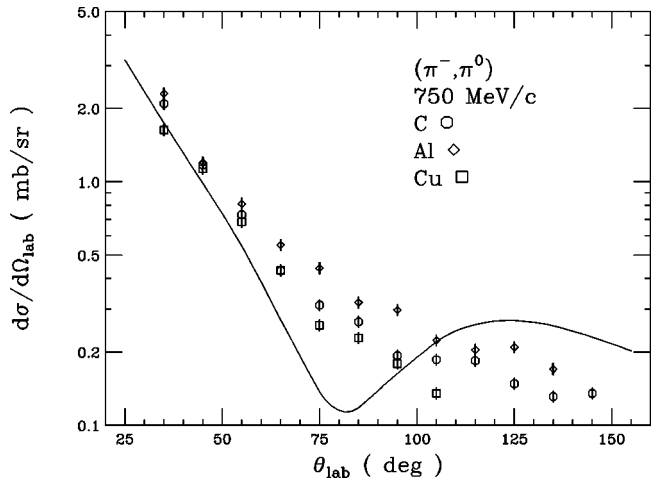

FIG. 6. Cross sections from fits to the SCX spectra with linear backgrounds such as shown in Figs. 2–4 subtracted are plotted, after division by Z_{eff}. The curve shows the free SCX cross sections [7], averaged over the same angle bins as the data. Note that the minimum near 75° in free space is lost for the complex targets. These cross sections without backgrounds agree with the relative values shown in Ref. [9].

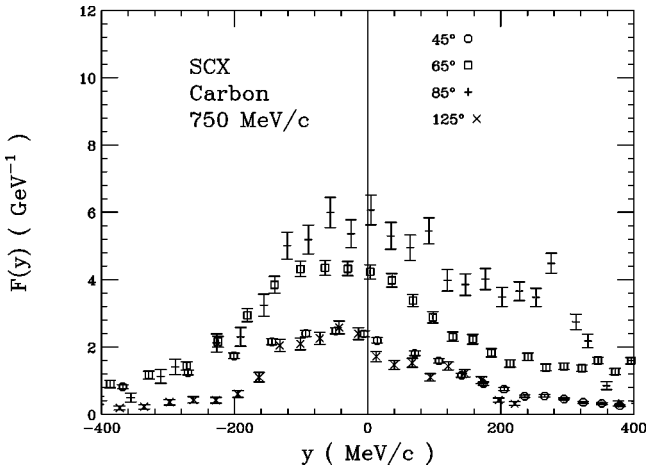

FIG. 7. Carbon SCX cross sections without background subtraction are shown transformed to the scaling response. The peak found near $y=0$ for these and other angles does not show a consistent scaling magnitude, and is not unidirectional with increasing angles.

in Fig. 7. The magnitudes of the $F(y)$ responses do not, however, scale together, and the peak is not found at $y=0$. This offset in energy (or y) was found to match closely the position of the measured free hydrogen SCX, indicating an inaccuracy of our absolute π^0 energy determination. This has almost no effect on the present analysis.

We next examine the possibility that the isovector SCX cross sections within the medium of our complex nuclear targets hold a different balance of spin-zero and spin-one transfer from those observed in free space, to account for the lack of scaling in magnitude.

IV. SPIN TRANSFER ANALYSIS

The sensitivity of the method developed here to separate $\Delta S=0$ and $\Delta S=1$ responses gains from the fact that the ratio of the $\Delta S=1$ differential cross section in free space to the total has a minimum near the middle of our angular range at 750 MeV/c [7], but not at the minimum of the differential cross section. The $\Delta S=1$ cross sections must vanish at 0° and 180° for the spin-zero mesons, but are also small near a laboratory angle of 65° for this momentum. The 4π coverage of the Crystal Ball ensures a large solid angle near mid-angles.

We create our spin separation by analogy to the Rosenbluth decomposition used for electron scattering. There, a form factor is defined by the ratio of measurements to the expectation for scattering from a single-point charge, that is with $\Delta S=0$ (longitudinal) scattering. When these form factors are plotted against a variable providing the relative $\Delta S=1$ (transverse) scattering to the $\Delta S=0$, the intercept and slope can be used to separate the $\Delta S=0$ and $\Delta S=1$ responses. The Rosenbluth parameter used is

$$x_R = \left(\tfrac{1}{2} + \tan^2\tfrac{\theta}{2}\right) \tag{6}$$

for the spin-1/2 electron. If the spin-zero meson could be treated in the same fashion, the separation variable would be $\tan^2\theta$, for $\Delta S=0$ scattering proportional to $\cos^2\theta$ and ΔS

$=1$ scattering proportional to $\sin^2\theta$. The spin transfer amplitudes for free π-nucleon scattering have been applied to π-nucleus coherent scattering [11]. There, an infinitely heavy nucleus was assumed ($\omega=0$), and data were plotted against beam energy for fixed q to recognize $\Delta S=0$ and $\Delta S=1$ transitions. A number of pion scattering experiments to discrete nuclear states used this simple separation to note the two spin possibilities [12].

Instead of simply the geometrical approximations, we here use the ratio of $\Delta S=1$ cross sections to $\Delta S=0$ cross sections directly from the phase-shift solution, using

$$x = |g|^2/|f|^2, \tag{7}$$

with g and f the $\Delta S=1$ and $\Delta S=0$ free-space amplitudes from Ref. [7]. The scaling responses $F(y)$ are used to plot $(1+x)\ F(y)$ against x to make our separation. We here use only the maxima of the observed responses above a background near $y=0$ from the fits as in Figs. 2–4. The statistical accuracy of the data is insufficient to use any other features of the spectra. Since recoil is important in our quasifree spectra, we use a fixed value (zero) of y, not q as used for nuclear transitions. For $\omega=0$, fixed q implies fixed y.

Measurements at 25° are not included in the fits or the plots, since their momentum transfers are not high enough to guarantee that the Pauli principle has not blocked the free scattering.

Further, by selecting the measurements near $y=0$ we minimize the role of the nucleons' internal motions. In the optimal frame description [13], just the laboratory energy is shown to be appropriate for hadron-nucleon scattering at $y=0$.

Results of this spin transformation are shown in Figs. 8 and 9 for three nuclear targets. Small values of x are found for small and large scattering angles, and near 65°. The largest values of x come from 105°. The straight line fits shown assume only that there is a single scaling response, here for its maximum, for $\Delta S=0$ (F_0) and for $\Delta S=1$ (F_1), but that these need not be equal to one another.

The fitted intercepts and slopes give the responses above backgrounds listed in Table II. For a simplest comparison, consider the intercept $F_0(y=0)=2.92(0.28)$ GeV^{-1} for carbon. Scattering from a Fermi gas with $k_F=235$ MeV/c would yield a parabolic shape for $F(y)$, centered at $y=0$ and extending between $y=-235$ MeV/c and $y=+235$ MeV/c. For this to have a unit area, corresponding to free scattering, the maximum would have to be 3.19 GeV^{-1}. Our observed $\Delta S=0$ maximum is near this value.

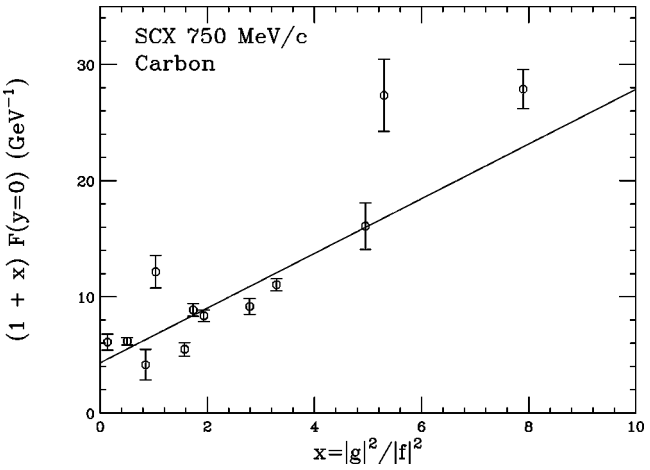

FIG. 8. The spin decomposition method developed in the text for spin-zero mesons provides the carbon data shown, for scattering angles from 35° to 145° at 750 MeV/c. The spin separation variable x is the ratio of spin to nonspin free-space cross sections, and only the fitted maxima (near $y=0$) of the cross sections above backgrounds such as shown in Fig. 2 are used. The intercept at $x=0$ is used to determine the nonspin response maximum, and the slope gives the spin response maximum.

The spin analysis indicates changes between $\Delta S=0$ and $\Delta S=1$ SCX cross sections in the medium from those in free space. These changes are thus seen to be responsible for the changes from the total free scattering differential cross sections noted in Fig. 6, and in the scaling of Fig. 7.

More thorough comparisons of these SCX spin-separated responses to other results will be provided in Sec. VI.

V. RESULTS FOR DEUTERIUM

The measurements included deuterium using the difference of spectra from a solid CD_2 target and a C sample. The

TABLE II. Maxima near $y=0$ of the spin-separated y-scaling functions $F(y=0)$ and the superscaling functions $f(Y=0)$, after subtraction of linear backgrounds as shown in Figs. 2–4, are compiled, as obtained from the linear fits shown in Figs. 8 and 9 for complex nuclei with 750 MeV/c pion SCX. These are compared to the maxima of the separated longitudinal (f_L) and transverse (f_T) superscaling functions read from Figs. 10 and 11 in Ref. [4], also with a linear background subtraction. Note that data from the same angular range were not available for all targets.

Nucleus	$F_0(y=0)$ (GeV^{-1})	$F_1(y=0)$ (GeV^{-1})	$f_0(Y=0)$	$f_1(Y=0)$	$f_L(Y=0)$	$f_T(Y=0)$
C	2.92(0.28)	2.04(0.15)	0.69(0.07)	0.48(0.04)	0.54(0.04)[a]	0.56(0.14)[a]
Al	4.91(0.31)	1.96(0.13)	1.13(0.07)	0.45(0.03)	0.50(0.04)[b]	0.48(0.16)[b]
Cu	3.99(0.35)	1.28(0.18)	1.11(0.10)	0.35(0.05)	0.50(0.04)[c]	0.41(0.20)[c]

[a]At $q=570$ MeV/c.
[b]For Ca at $q=570$ MeV/c.
[c]For Fe at $q=570$ MeV/c.

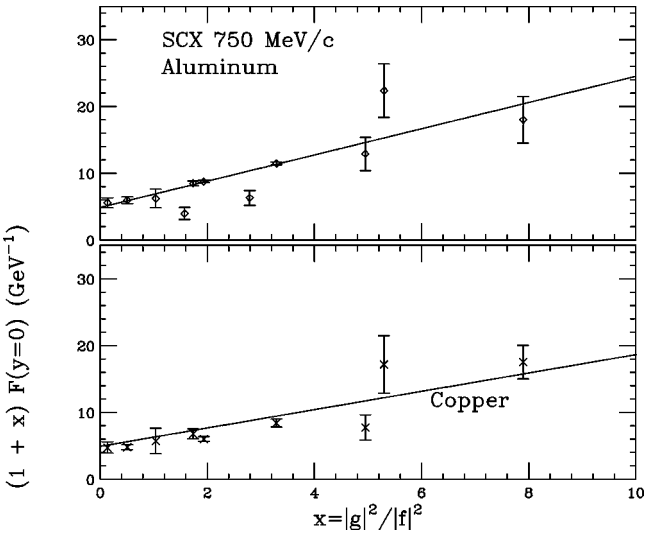

FIG. 9. As for Fig. 8, but for the Al and Cu samples.

narrow quasifree peak in the doubly differential cross sections seen in Fig. 10 provided a reliable area to determine the single-differential cross section, in contrast to the data including a continuum background for the complex nuclei. These data transformed to the *y*-scaling format are also shown in Fig. 11. A value of $Z_{\mathrm{eff}}=1$ is used for this analysis; our Glauber model gives an expectation very near unity.

Figure 12 shows the deuteron π^- SCX cross sections, with comparisons to the expectations from the phase-shift analysis. The curve is averaged over the same angle bins as are the deuteron data. The differences from free scattering are similar to, but less marked, than seen for the heavier nuclei in Fig. 6. See also the results in Ref. [14] for 624 MeV/c SCX.

The spin decomposition for deuterium is applied to the areas, and not just to the maxima of the scaling responses, in order to garner more counts for better accuracy. Differential cross-section ratios to data for protons are used in Fig. 13, with the linear best fit. The intercept and the slope give ratios to free scattering of 1.37(0.07) for $\Delta S=0$ and 0.77(0.04) for $\Delta S=1$.

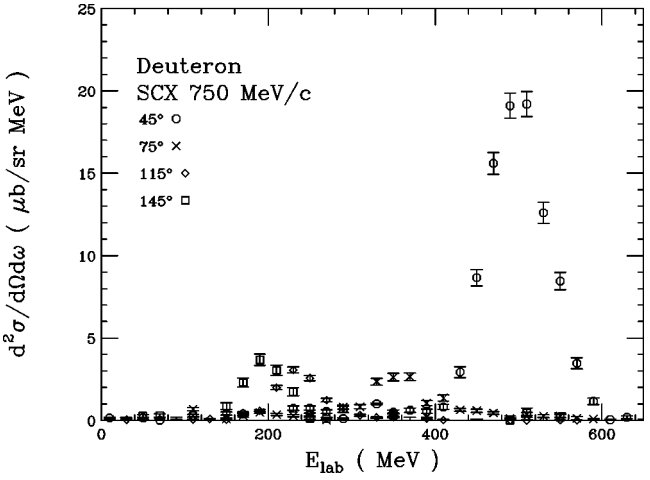

FIG. 10. Samples of doubly differential cross sections for $D(\pi^-,\pi^0)$ at 750 MeV/c. Note the lack of backgrounds.

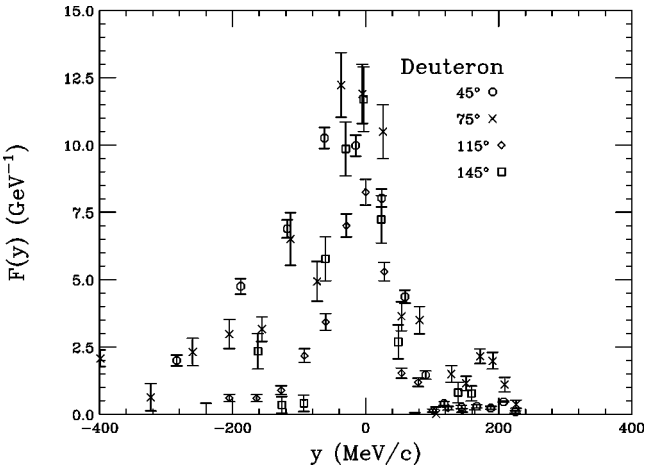

FIG. 11. Pion SCX cross sections shown in Fig. 10 are here shown in the *y*-scaling format. The recoil correction approximation in Eq. (1) is very large for this case.

An extrapolation to $x=0$ at 180° using only deuteron SCX data from 105° to 155° provides a ratio to the hydrogen SCX data of 0.94(0.10). This indicates little if any change in the isovector $\Delta S=0$ strength at $q=1028$ MeV/c ($Q^2=q^2-\omega^2=0.83$ GeV^2). This information for $\Delta S=0$ is complementary to isovector electron scattering data sensitive to the $\Delta S=1$ strength in deuterium at similar momentum transfers [15].

VI. COMPARISONS OF RESPONSES AND CONCLUSIONS

Since we are using a strongly interacting probe of a nuclear response, the effects of nuclear absorption, shadowing, and multiple interactions must be treated and shown to be known to sufficient accuracy to use the nuclear response results. The Glauber method [6] used here was shown in Fig. 5 to yield the superscaling response at a single angle for our range of nuclear target masses. In Ref. [2] it was shown that

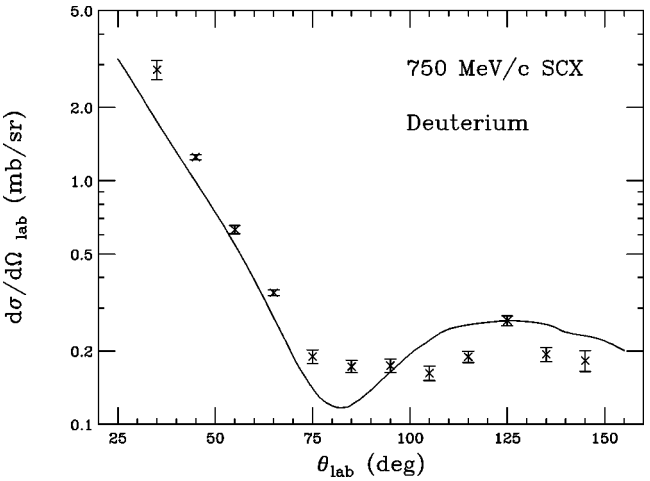

FIG. 12. Integrated quasifree cross sections for $D(\pi^-,\pi^0)$ are shown for 750 MeV/c, compared to free-space expectations [7], averaged over the same angle bins as the data.

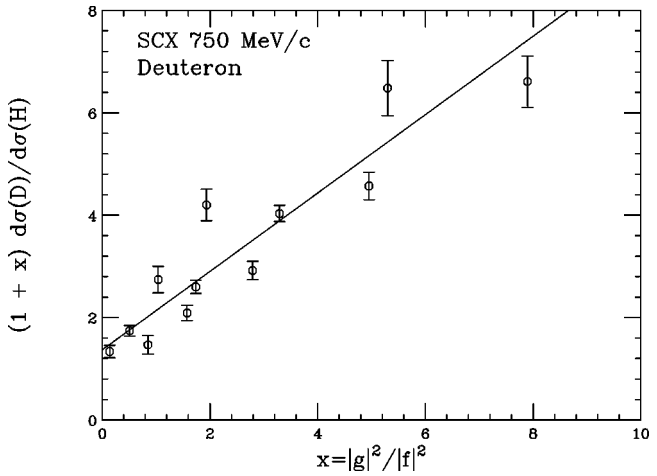

FIG. 13. Areas of the *y*-scaling response functions observed for deuterium are used for a spin separation similar to that used for the heavier nuclear targets. Free scattering would yield an intercept and a slope each equal to unity.

this model also reproduces π^--carbon total cross sections to about the same accuracy as the scatter seen here in Fig. 5. We concude that the $Z_{\rm eff}$ approximation is valid for our analysis.

The assumption of one and only one quasifree interaction between the pion projectile and ejectile with target nucleons is tested by the kinematics of the *y*-scaling transformation. The 750 MeV/*c* Crystal Ball data shown here are selected from π^0 decays into two photons only, and strongly exclude inelastic events. An analysis of $2\pi^0$ events is found in Ref. [9]. We find the exclusive (π^-,π^0) spectra to show evidence of *y* scaling in Fig. 7, in that the expected quasifree response peak very near the energy for free SCX is obtained over a wide range of angles, from $q=430$ MeV/*c* to $q=1004$ MeV/*c* for carbon. The magnitudes of these responses do not scale, however. A similar situation was found for nuclear *y*-scaling studies of pion NCX at 950 MeV/*c* [2], with better agreement as *q* was changed than is seen here.

We ascribe the failure to scale in the 750 MeV/*c* Crystal Ball data to a change in the pion-nucleon differential cross sections within the complex targets. A new method to separate the spin-zero and spin-one transfer responses was presented, and shown to provide the straight line fits shown in Figs. 8 and 9. The angular dependence of the ratio of spin to nonspin free SCX cross sections at 750 MeV/*c* and the full angular range offered by the Crystal Ball detector enable this method to be quite sensitive. The separated maxima of the *y*-scaling responses for C, Al, and Cu, as listed in Table II, indeed differ for $\Delta S=0$ and $\Delta S=1$.

The SCX *y*-scaling responses are best compared to separated electron scattering responses by the superscaling format, using Figs. 10 and 11 of Ref. [4]. Peak magnitudes above linear backgrounds were estimated for the electron data, as was done with our SCX results. We use the Fermi momenta from Table I to compute the $f(Y=0)$ SCX superscaling maxima in Table II. The $\Delta S=0$ pion quasifree SCX isovector maxima f_0 are larger than the longitudinal f_L or $\Delta S=0$ charge responses, due only to the charge of the protons in the targets. Our SCX responses are also from target protons. Pion NCX studies showed an enhancement in the nuclear medium of the isoscalar $\Delta S=0$ cross sections [2]. If the small $\Delta S=1$ cross sections for π^- NCX at 950 MeV/*c* and K^+ at 705 MeV/*c* and $q=500$ MeV/*c* are not included, these NCX data [10] would provide values of f_0 near unity. Thus the nearly isoscalar NCX and the strictly isovector SCX superscaling maxima agree quite well in the $\Delta S=0$ channel, and both exceed the measured charge response f_L.

The isovector responses from pion SCX are more directly comparable to the transverse electromagnetic data, predominantly also isovector. The $\Delta S=1$ transfer by the spin-zero pion must also be transverse to the direction of the momentum transfer. The pion response maxima above backgrounds are found to be smaller than those from electron scattering, although the cases cannot be compared directly. If electron and pion SCX data without backgrounds are compared, the comparisons of $\Delta S=0$ and $\Delta S=1$ responses are much the same as obtained here with backgrounds for each. The pion SCX data cover about twice the range of momentum transfer *q* as the electron data in Figs. 10 and 11 of Ref. [4].

These evidences of a medium effect altering pion SCX cross sections in nuclei from their free-space values will need to be considered in light of recent theoretical understandings; a list of relevant references is given in Ref. [9]. Smaller in-medium $\Delta S=1$ SCX cross sections and larger in-medium $\Delta S=0$ SCX cross sections are implied by the separated scaling responses in Table II, in order to bring agreement between pion and electron data for SCX on deuterium and complex nuclei.

It is the large angular acceptance and specific single π^0 triggering available with the Crystal Ball detector that enables this work to make a quantitative study of pion quasifree SCX *y*-scaling, and to enable the new $\Delta S=0$ and $\Delta S=1$ separation that permits a most useful comparison between electromagnetic and hadronic means to study nuclear *y*-scaling responses.

ACKNOWLEDGMENTS

This work was supported in part by the U.S. DOE, the U.S. NSF, the Croatian Ministry of Science, the Russian Foundation for Basic Research, the Russian Ministry of Industry, Science, and Technologies, NSERC of Canada, the G.W. Research Enrichment Fund, and the Volkswagen Stiftung.

[1] D. B. Day, J. S. McCarthy, T. W. Donnelly, and I. Sick, Annu. Rev. Nucl. Part. Sci. **40**, 357 (1990).
[2] R. J. Peterson *et al.*, Phys. Rev. C **65**, 054601 (2002).
[3] M. L. Goldberger and K. M. Watson, *Collision Theory* (Wiley, New York, 1964).
[4] T. W. Donnelly and I. Sick, Phys. Rev. C **60**, 065502 (1999).
[5] S. W. Hong and B. T. Kim, J. Phys. G **25**, 1065 (1999).
[6] J. Ouyang. S. Hoibraten, and R. J. Peterson, Phys. Rev. C **47**, 2809 (1993).
[7] R. A. Arndt *et al.*, Phys. Rev. C **56**, 3005 (1997); Scattering Analysis Interactive Dialin (SAID), solution SM95, http://gwdac.phys.gwu.edu/
[8] J. D. Patterson and R. J. Peterson, Nucl. Phys. **A717**, 235 (2003).
[9] A. B. Starostin *et al.*, Phys. Rev. C **66**, 055205 (2002).
[10] R. J. Peterson *et al.*, Phys. Lett. B **297**, 238 (1992).
[11] E. R. Siciliano and G. E. Walter, Phys. Rev. C **23**, 2661 (1981).
[12] D. B. Holtkamp *et al.*, Phys. Rev. C **31**, 957 (1985).
[13] S. A. Gurvitz, Phys. Rev. C **33**, 422 (1986).
[14] R. J. Peterson, J. Ouyang, S. Hoibraten, and L. B. Weinstein, Phys. Rev. C **52**, 33 (1995).
[15] H. J. Bulten *et al.*, Phys. Rev. Lett. **74**, 4775 (1995).